

## Subunit rotation in *Escherichia coli* F<sub>0</sub>F<sub>1</sub>-ATP synthase during oxidative phosphorylation

YUANTAI ZHOU, THOMAS M. DUNCAN, AND RICHARD L. CROSS\*

Department of Biochemistry and Molecular Biology, State University of New York Health Science Center, 750 East Adams Street, Syracuse, NY 13210

Communicated by Paul D. Boyer, University of California, Los Angeles, CA, July 29, 1997 (received for review May 21, 1997)

**ABSTRACT** We report evidence for proton-driven subunit rotation in membrane-bound F<sub>0</sub>F<sub>1</sub>-ATP synthase during oxidative phosphorylation. A  $\beta$ D380C/ $\gamma$ C87 crosslinked hybrid F<sub>1</sub> having epitope-tagged  $\beta$ D380C subunits ( $\beta_{\text{flag}}$ ) exclusively in the two noncrosslinked positions was bound to F<sub>0</sub> in F<sub>1</sub>-depleted membranes. After reduction of the  $\beta$ - $\gamma$  crosslink, a brief exposure to conditions for ATP synthesis followed by reoxidation resulted in a significant amount of  $\beta_{\text{flag}}$  appearing in the  $\beta$ - $\gamma$  crosslinked product. Such a reorientation of  $\gamma$ C87 relative to the three  $\beta$  subunits can only occur through subunit rotation. Rotation was inhibited when proton transport through F<sub>0</sub> was blocked or when ADP and P<sub>i</sub> were omitted. These results establish F<sub>0</sub>F<sub>1</sub> as the second example in nature where proton transport is coupled to subunit rotation.

F<sub>0</sub>F<sub>1</sub>-ATP synthases are found embedded in the membranes of mitochondria, chloroplasts, and bacteria, and are structurally and functionally conserved among species (1–5). During oxidative- and photo-phosphorylation, the synthases couple the movement of protons down an electrochemical gradient to the synthesis of ATP. The F<sub>0</sub> sector is composed of membrane-spanning subunits (ab<sub>2</sub>c<sub>9–12</sub> in *Escherichia coli*) that conduct protons across the membrane, whereas the F<sub>1</sub> sector ( $\alpha_3\beta_3\gamma\delta\epsilon$ ) is an extrinsic complex that contains the catalytic sites for ATP synthesis. F<sub>1</sub> can be removed from the membrane in a soluble form that functions as an ATPase, and rebinding F<sub>1</sub> to F<sub>0</sub> in membranes restores the capacity to catalyze net ATP synthesis. A high-resolution structure of bovine F<sub>1</sub> shows a hexamer of alternating  $\alpha$  and  $\beta$  subunits surrounding a single  $\gamma$  subunit. The three catalytic sites of F<sub>1</sub> are located on the three  $\beta$  subunits at  $\alpha/\beta$  subunit interfaces (6).

The model for energy coupling by F<sub>0</sub>F<sub>1</sub>-ATP synthases that has gained the most general support is called the binding change mechanism (7). According to this proposal, the major energy requiring step (Fig. 1*a*, step 1) is not the synthesis of ATP at catalytic sites, but rather the simultaneous and highly cooperative binding of substrates to, and release of products from, these sites (14, 15). Furthermore, it is proposed that these affinity changes are coupled to proton transport by the rotation of a complex of subunits that extends through F<sub>0</sub>F<sub>1</sub>. Rotation of the  $\gamma$  subunit in the center of F<sub>1</sub> (Fig. 1*a*) is thought to deform the surrounding catalytic subunits to give the required binding changes (16), whereas rotation of the c-subunits relative to the single a-subunit in F<sub>0</sub> (Fig. 1*b*) is believed to be required for completion of the proton pathway (8, 17, 18). The latter is analogous to the proton-driven subunit rotation that occurs within the bacterial flagellar motor (19).

Based on supportive evidence from several laboratories (6, 16, 20, 21), the rotary aspect of the binding change mechanism has remained a popular idea. However, a critical test for rotation only became possible recently. The crystal structure of

bovine mitochondrial F<sub>1</sub> shows a specific interaction between a small  $\alpha$ -helix of the  $\gamma$  subunit, which contains a Cys (*E. coli*  $\gamma$ C87), and the “DELSEED” loop of one of the three  $\beta$  subunits (6). We substituted Cys for several different residues in this region of *E. coli*  $\beta$  (<sub>380</sub>DELSEED<sub>386</sub>) and found that the presence of an oxidant induced rapid and specific formation of a  $\beta$ D380C- $\gamma$ C87 disulfide bond in  $\beta$ D380C-F<sub>1</sub> (8, 22). Using a dissociation/reassociation approach with the  $\beta$ - $\gamma$  crosslinked  $\beta$ D380C-F<sub>1</sub>, we incorporated radiolabeled  $\beta$  subunits into the two noncrosslinked  $\beta$  subunit positions of F<sub>1</sub>. Following reduction of the crosslink and a short burst of ATP cleavage, radiolabeled and unlabeled  $\beta$  subunits in the hybrid F<sub>1</sub> showed a similar capacity to form a disulfide bond with the  $\gamma$  subunit (8), indicating that  $\gamma$  rotates relative to  $\beta$  subunits during ATP hydrolysis. We then showed that hybrid F<sub>1</sub> containing a  $\beta$ D380C- $\gamma$ C87 crosslink can be recoupled to F<sub>0</sub> in F<sub>1</sub>-depleted membranes and we provided evidence that rotation of  $\gamma$  relative to  $\beta$  subunits also occurs during hydrolysis of ATP by F<sub>0</sub>F<sub>1</sub> (23). Subsequently, additional evidence for subunit rotation during ATP hydrolysis was provided by using immobilized chloroplast F<sub>1</sub> with a spectroscopic probe attached near the C terminus of the  $\gamma$  subunit. Recovery of polarized absorption after photobleaching was used to monitor rotational motion of  $\gamma$  during ATP hydrolysis by the tethered F<sub>1</sub> (24). In a more recent study using immobilized bacterial F<sub>1</sub>, a fluorescent actin filament was attached to one end of the  $\gamma$  subunit and fluorescence microscopy was used to monitor its rotation during catalytic turnover (25). It was shown that MgATP could induce net unidirectional rotation of  $\gamma$  through many complete revolutions. However, studies thus far have not examined whether rotation of F<sub>1</sub> subunits occurs in coupled F<sub>0</sub>F<sub>1</sub> during the physiologically important reaction of ATP synthesis. We now extend our hybrid F<sub>1</sub>/crosslinking approach to provide the first clear indication that subunit rotation in F<sub>0</sub>F<sub>1</sub> is an integral part of energy coupling during oxidative phosphorylation.

### MATERIALS AND METHODS

**Materials.** NADH, *N,N'*-dicyclohexylcarbodiimide (DCCD), carbonylcyanide *p*-trifluoro-methoxyphenylhydrazone (FCCP), *N*-ethylmaleimide (NEM), ATP, ADP, selenocystamine, and hexokinase were supplied by Sigma, 5,5'-dithiobis(2-nitrobenzoate) (DTNB) by Aldrich, DTT by American Bioanalytical (Natick, MA), lauryldimethylamine oxide (LDAO) by Calbiochem, [ $\gamma$ -<sup>32</sup>P]ATP by ICN, anti-Flag M2 antibody by Eastman Kodak, and anti-mouse IgG/alkaline phosphatase conjugate by Promega. Alkaline phosphatase color development reagents were from Bio-Rad, pyruvate kinase and lactate dehydrogenase from Boehringer Mannheim, and polyvinylidene difluoride (PVDF) membranes from NOVEX (San Diego). Other reagents and chemicals were the highest grade available.

Abbreviation: DCCD, *N,N'*-dicyclohexylcarbodiimide.  
\*e-mail: crossr@vax.cs.hscsyr.edu.

The publication costs of this article were defrayed in part by page charge payment. This article must therefore be hereby marked “advertisement” in accordance with 18 U.S.C. §1734 solely to indicate this fact.

© 1997 by The National Academy of Sciences 0027-8424/97/9410583-5\$2.00/0  
PNAS is available online at <http://www.pnas.org>.

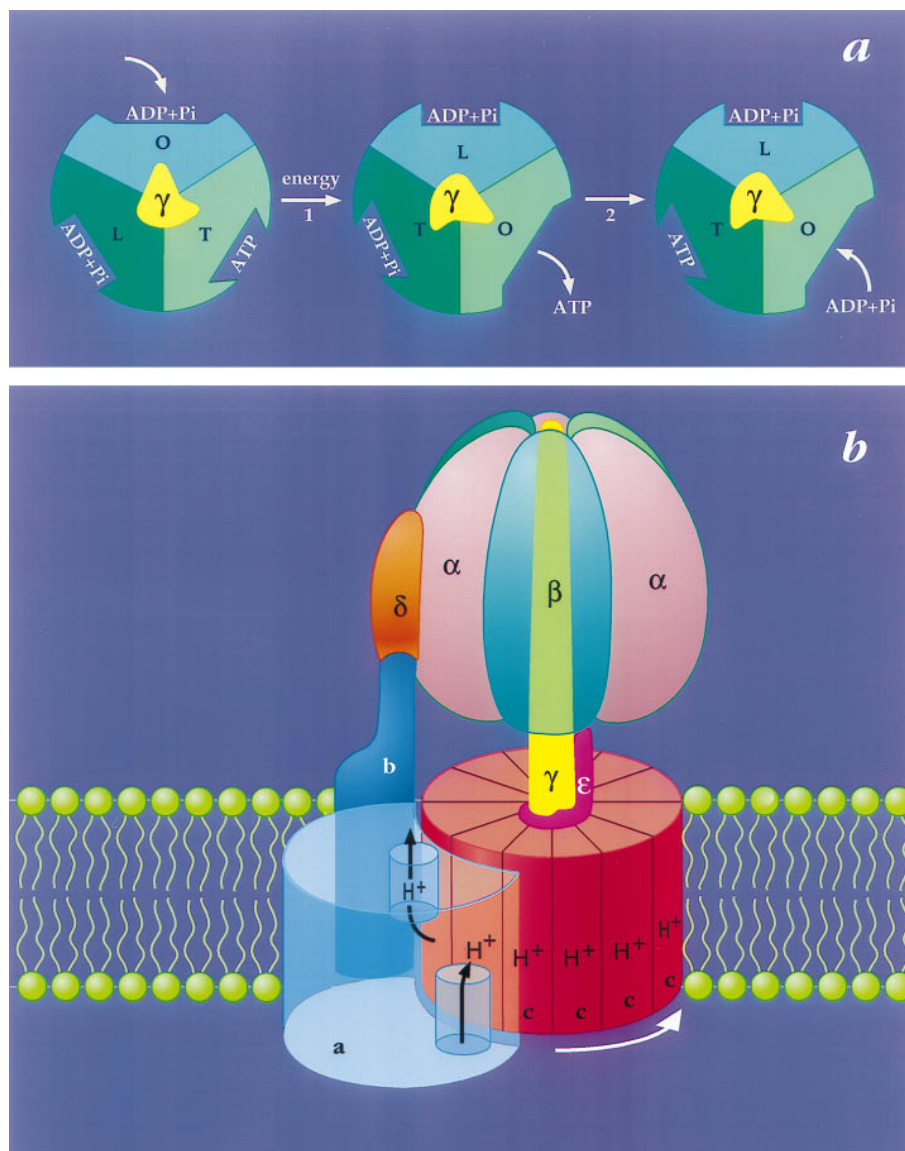


FIG. 1. The binding change mechanism for  $F_0F_1$  ATP synthases. This figure was adapted from ref. 8 and modified. (a) Looking up at  $F_1$  from the membrane. In step 1, the asymmetric  $\gamma$  subunit rotates  $120^\circ$  clockwise driving conformational changes in the three catalytic sites that alter their affinities for substrates and product. In this illustration, the catalytic sites remain stationary. In step 2, ATP forms spontaneously from tightly bound ADP and  $P_i$ . For additional details and alternative views see refs. 7, 9, and 10. (b) View from the side of  $F_0F_1$ . The a-subunit contains two partial channels, each in contact with a different side of the membrane. In order for a  $H^+$  to traverse the membrane it moves through one channel to the center of the membrane, binds to one of the c-subunits (at Asp-61), and then is carried to the other partial channel by rotation of the c-subunit complex. The c-subunits are anchored to  $\gamma$  (11), whereas the a-subunit is anchored through subunits b and  $\delta$  to the periphery of the  $\alpha_3\beta_3$  hexamer (12, 13). Hence the rotation of c-subunits relative to the a-subunit in  $F_0$  will drive the rotation of  $\gamma$  relative to the  $\alpha_3\beta_3$  hexamer in  $F_1$ .

**Plasmids and *E. coli* Strains.** Plasmids p3U and pAU1, and mutants  $\beta D380C$  and  $\beta_{flag}D380C/\gamma C87S$  have been reported (22, 23). Mutant  $\beta D380C-F_1$  was expressed in strain JP17, which has a chromosomal deletion of most of the *uncD* gene coding for the  $\beta$  subunit (26). Mutant  $\beta_{flag}D380C/\gamma C87S-F_1$  was expressed in strain AN887, which has a Mu insertion that blocks expression of all *unc* genes from the chromosome (27).

**Preparation of *E. coli* Membranes and Soluble  $F_1$ .** Membranes were isolated and washed (28, 29) and soluble  $F_1$  was purified (8) as described. Membranes prepared from strain JP17 harboring pAU1 were depleted of  $F_1$  (28) with two additional washes with 10 mM Tris-acetate/1 mM EDTA, pH 7.5.

**Preparation of Hybrid  $F_1$  and Reconstitution with  $F_1$ -Depleted Membranes.**  $\beta D380C-F_1$  was treated with DTNB to induce disulfide bond formation between  $\gamma C87$  and the  $\beta D380C$  of one  $\beta$  subunit (8). The crosslinked enzyme and  $\beta_{flag}D380C/\gamma C87S-F_1$  were then treated under conditions that

cause disassembly of subunits, mixed in a 1:1 ratio, and allowed to reassemble as hybrid  $F_1$  complexes as described previously (8).  $F_1$  hybrids that contain  $\beta D380C-\gamma C87$  can contain  $\beta_{flag}D380C$  subunits only in the two noncrosslinked  $\beta$  positions.  $F_1$  hybrids containing the  $\gamma C87S$  subunit can contain  $\beta_{flag}D380C$  in any of the three  $\beta$  positions, but these hybrids will be incapable of forming a  $\beta-\gamma$  disulfide bond due to the  $\gamma C87S$  mutation. However, oxidation of  $F_1$  containing  $\beta D380C$  and  $\gamma C87S$  can yield low levels of a 101-kDa crosslinked product previously identified as a  $\beta-\beta$  dimer (ref. 8; see Fig. 2). Hybrid  $F_1$  (0.5 mg/ml) was recoupled to  $F_0$  in  $F_1$ -depleted membranes (2 mg protein per ml) by incubation in TMg buffer (50 mM Tris-acetate/10 mM  $MgSO_4$ , pH 7.5) at  $30^\circ C$  for 15 min. Unbound  $F_1$  was removed by centrifuging at  $100,000 \times g$  in a Beckman Airfuge for 1 min. The membrane pellet was resuspended and washed twice with TSGMg buffer (50 mM Tris-acetate/250 mM sucrose/50 mM glucose/5 mM

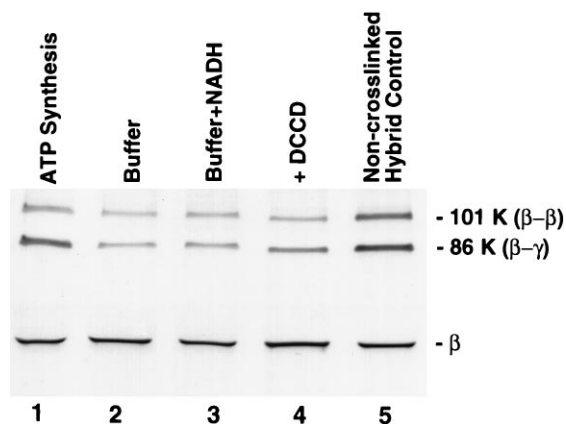


FIG. 2. Rotation of subunits in *E. coli*  $F_0F_1$  under ATP synthesis conditions. Hybrid  $F_1$  was prepared so that complexes containing a  $\beta D380C/\gamma C87$  crosslink contained  $\beta_{flag}D380C$  subunits only in the two noncrosslinked  $\beta$  positions. After rebinding hybrid  $F_1$  to  $F_1$ -depleted membranes, aliquots (1 mg total protein per ml) were exposed to different conditions (described below) for 30 sec at 23°C, 20 mM DTT and 2 mM selenocystamine were added to rapidly reduce any disulfide bonds, and the membranes were incubated for an additional 30 sec before passage through a Sephadex G50-F centrifuge column (30), equilibrated with TSGMg buffer. Disulfide bond formation was induced as each sample eluted from the column into a tube containing DTNB (0.2 mM final concentration). An aliquot of each oxidized sample (equivalent to 0.4  $\mu g$  of  $\beta_{flag}-F_1$ ) was denatured under nonreducing conditions and used for SDS/PAGE and immunoblotting. The blot above shows bands containing the  $\beta_{flag}D380C$  subunit. As shown in lanes 1–4, membranes were exposed to the following conditions: lane 1, conditions for ATP synthesis (TSGMg buffer containing 4 mM ADP/20 mM  $P_i$ /2 mM NADH/165 units hexokinase/ml); lane 2, same as for lane 1 except that ADP,  $P_i$ , and NADH were omitted; lane 3, same as for lane 1 except that ADP and  $P_i$  were omitted; lane 4, same as for lane 1 except that  $F_1$ -depleted membranes were pretreated with DCCD prior to reconstitution with hybrid  $F_1$  (see *Materials and Methods*). For the “noncrosslinked hybrid” control in lane 5, hybrid  $F_1$  was prepared from dissociated subunits without prior crosslinking of  $\gamma C87$  to a  $\beta D380C$  subunit. Thus, epitope-tagged  $\beta$  subunit could assemble randomly in the three  $\beta$  positions around the  $\gamma C87$  subunit. After rebinding to membranes and exposure to ATP synthesis conditions (as for lane 1), reoxidation of this sample provided a measure of the amount of  $\beta_{flag}D380C$  trapped in the  $\beta$ - $\gamma$  crosslinked product when the orientation of  $\gamma C87$  is random relative to the three  $\beta$  positions.

$MgSO_4$ , pH 7.4) and finally resuspended in the same buffer at 4 mg protein per ml.

**DCCD Modification of  $F_0$ .**  $F_1$ -depleted membranes (2 mg protein per ml) were incubated with 100  $\mu M$  DCCD in TMg buffer at 0°C for 20 hr with slow stirring. Membranes were sedimented by centrifuging at 100,000  $\times g$  in an Airfuge for 1 min, washed twice with TMg buffer, and resuspended in the same buffer at 4 mg protein per ml.

**ATP Synthesis Assay.** The ATP synthesis activity of reconstituted membranes was determined as the rate of glucose-6- $^{32}P$  formation. Each 250- $\mu l$  aliquot contained 25  $\mu g$  of membrane protein in TSGMg buffer with 4 mM ADP, 20 mM  $^{32}P_i$ , and 40 units of hexokinase. After preincubation at 23°C for 5 min, ATP synthesis was initiated by adding NADH (2 mM final concentration). Each timed sample was quenched by adding 25  $\mu l$  of 5.5 M perchloric acid.  $P_i$  was precipitated (31) and glucose-6- $^{32}P$  in the supernatant was determined by Cerenkov counting. No significant ATP synthesis was detected in the presence of uncoupler (55  $\mu M$  FCCP), and pretreatment of membranes with DCCD before reconstitution with  $F_1$  inhibited ATP synthesis by 92%. In a control experiment for the hexokinase trap, no detectable  $^{32}P_i$  was produced when 1  $\mu M$  [ $\gamma$ - $^{32}P$ ]ATP was incubated

with 50 units of hexokinase plus 100  $\mu g$  of reduced, reconstituted membranes in 1 ml of TSGMg buffer.

**Electrophoresis and Immunological Detection of Proteins Containing the Flag Epitope.** SDS/PAGE (32) was performed on 4–15% acrylamide gradient gels (Ready gels, Bio-Rad). For nonreducing conditions, samples were denatured in the presence of 0.5 mM NEM instead of 2-mercaptoethanol. Proteins were transferred from the gel to a PVDF membrane at 250 mA for 90 min in 25 mM Tris/192 mM glycine/10% methanol/0.005% SDS (33). The blotted membrane was blocked with 5% nonfat, dried milk in TBST (10 mM Tris-HCl/150 mM NaCl/0.05% Tween-20, pH 8.0) and incubated with anti-Flag M2 antibody (0.4  $\mu g/ml$  in TBST), then rinsed three times with TBST + 0.1 M NaCl. Bands containing the Flag epitope were then visualized colorimetrically using a secondary-antibody/alkaline phosphatase conjugate and quantitated using a Hewlett–Packard scanner (model C2501) and densitometry software from Biosoft (Milltown, NJ). Known amounts of  $\beta_{flag}-F_1$  were run on a separate gel in the presence of 2-mercaptoethanol, blotted, and the Flag epitope in the  $\beta$ -subunit band of each sample was quantitated as described above. The results showed a range for which densitometry had a linear dependence on the amount of protein added. This provided a standard curve for determining the total  $\beta_{flag}$  in aliquots of each experimental sample run on a preliminary reducing gel, so that aliquots containing identical amounts of  $\beta_{flag}$  could be added to each lane of a nonreducing gel.

**Protein Assay.** Protein concentrations were determined by a modified Lowry assay (34).

## RESULTS AND DISCUSSION

$F_1$ -depleted membranes were reconstituted with hybrid  $F_1$  that contained a  $\beta D380C-\gamma C87$  disulfide crosslink with epitope-tagged  $\beta_{flag}D380C$  subunits only at the two noncrosslinked  $\beta$  positions. Following reduction of the intersubunit disulfide, these reconstituted membranes were capable of catalyzing electron transport-driven ATP synthesis at a rate of 87  $nmol \cdot min^{-1} \cdot mg^{-1}$  membrane protein. To test for subunit rotation during ATP synthesis, the reconstituted membranes were reduced, incubated briefly under conditions for ATP synthesis, and then reoxidized. To preclude any contribution of ATP hydrolysis to subunit rotation under these conditions, hexokinase and glucose were present to trap ATP synthesized by  $F_0F_1$  (see *Materials and Methods*). In the absence of subunit rotation,  $\gamma C87$  would be expected to reform a disulfide link to the original  $\beta D380C$  and thus the Flag epitope would not be detected in the  $\beta$ - $\gamma$  crosslinked product (an 86-kDa band) on an immunoblot. However, if subunit rotation occurred during ATP synthesis, as predicted by the binding change mechanism (Fig. 1), then  $\beta_{flag}D380C$  would be properly aligned to crosslink to  $\gamma C87$  in two-thirds of the  $F_0F_1$  hybrid molecules containing  $\gamma C87$ . Fig. 2 shows that exposure to ATP synthesis conditions resulted in a significant amount of Flag epitope in the  $\beta$ - $\gamma$  band (lane 1), demonstrating that subunit rotation had occurred. In contrast, when ADP,  $P_i$ , and NADH were omitted, much less  $\beta_{flag}$  was detected in the  $\beta$ - $\gamma$  band (lane 2).

The binding change mechanism stipulates that ADP and  $P_i$  must bind at a catalytic site on  $F_1$  before protons can be transported through  $F_0$  down an electrochemical gradient. If these two events were not sequentially linked and proton transport could drive subunit rotation when catalytic sites were empty, energy would be wasted. The existence of this obligatory coupling is clearly demonstrated in Fig. 2 where, in the absence of ADP and  $P_i$ , the presence of NADH resulted in little  $\beta_{flag}$  in the  $\beta$ - $\gamma$  band (lane 3). This indicates that an electrochemical gradient alone is not sufficient to

promote subunit rotation in  $F_0F_1$ ; ADP and  $P_i$  must also be present.

Transport of protons through  $F_0$  can be blocked by covalent modification of one or more c-subunits with DCCD, and this also blocks ATP synthesis or hydrolysis by  $F_0F_1$  (35). When  $F_1$ -depleted membranes were treated with DCCD prior to reconstitution with hybrid  $F_1$ , exposure of reconstituted membranes to ATP synthesis conditions, as for lane 1, showed considerably reduced amounts of  $\beta_{\text{flag}}$  in the  $\beta$ - $\gamma$  band (Fig. 2, lane 4), indicating that subunit rotation in  $F_1$  is blocked by modifying  $F_0$  with DCCD.

The amount of Flag epitope observed in the  $\beta$ - $\gamma$  crosslinked product was quantitated and compared with that expected if the orientation of  $\gamma$  was randomized during turnover relative to the three surrounding  $\beta$  subunits and if 100% of the  $F_0F_1$ -ATP synthase complexes present in the membranes were catalytically active during the brief episode of ATP synthesis (Fig. 3). Conditions for ATP synthesis yielded 76% of this expected value, a reasonable correlation considering the probability that a fraction of  $F_0F_1$  is bound to leaky or uncoupled membranes and would thus remain inactive and immobile during the experiment. In contrast, controls lacking NADH and/or ADP and  $P_i$  had only 17–21% of the expected value (Fig. 3, Buffer and Buffer+NADH). Furthermore, when  $F_1$ -depleted membranes were treated with DCCD prior to binding hybrid  $F_1$ , exposure to ATP synthesis condition yielded only 35% of the expected  $\beta_{\text{flag}}$  in the 86-kDa band (Fig. 3, +DCCD). This emphasizes the tight functional linkage of  $F_0$  to subunit rotation in  $F_1$ , and supports the plausibility of subunit rotation in  $F_0$ .

Previously, the bacterial flagellar motor was the only macromolecular complex known to use an electrochemical proton gradient to drive subunit rotation (19). The results presented in Figs. 2 and 3 provide strong support for the conclusion that the  $F_0F_1$ -ATP synthase is a second example. The recent visual observation of net unidirectional rotation during ATP hydrolysis by  $F_1$  (25) suggests the sequential participation of all three catalytic sites and that the direction of rotation will depend on whether it is driven by ATP hydrolysis or proton transport. In view of the close evolutionary relationship between  $F_0F_1$  synthases and the  $V_0V_1$  ATPases (36), it seems likely that the acidification of vacuoles also requires subunit rotation. In addition, it is becoming apparent that RecA (37, 38) and DNA

and RNA helicases (38–40) may operate by a rotary-type mechanism. In analogy to the rotation of  $\gamma$  within the  $\alpha_3\beta_3$  hexamer of  $F_1$ , a single strand of DNA or RNA is thought to rotate within a hexamer of subunits which show clear structural homologies with the  $F_1$ - $\beta$  subunit (6, 41–43). Whereas RecA and the helicases use ATP hydrolysis to drive rotation and the flagellar motor uses an electrochemical gradient,  $F_0F_1$ -ATP synthases appear to be unique in that they can use either. Thus, further analysis of rotational coupling in  $F_0F_1$  may provide useful insights for these diverse systems.

We wish to thank Marcus L. Hutcheon for excellent technical assistance. This work was supported by Research Grant GM23152 from the National Institutes of Health, U.S. Public Health Service.

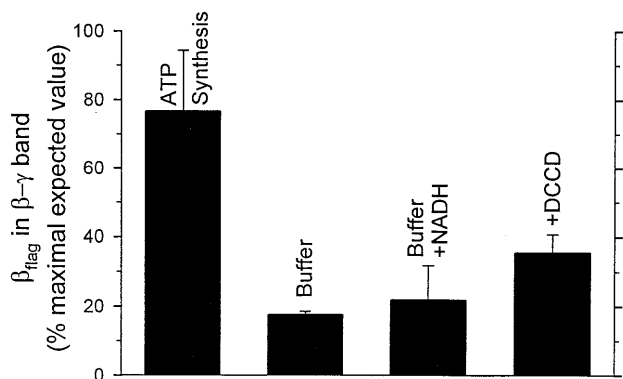


Fig. 3. Quantitation of the Flag epitope appearing in the  $\beta$ - $\gamma$  crosslinked product. For immunoblots as in Fig. 2, the amount of  $\beta_{\text{flag}}$  in the 86-kDa band of each sample was determined by scanning densitometry. The value obtained for a “noncrosslinked hybrid” control (see Fig. 2, lane 5) was multiplied by 0.8 to correct for its greater  $\beta_{\text{flag}}$  content compared with the crosslinked hybrid  $F_1$  (Fig. 2, lanes 1–4). This value was set to 100%, representing the amount of  $\beta_{\text{flag}}$  expected in the  $\beta$ - $\gamma$  crosslinked product if each  $\beta$  subunit has an equal opportunity to crosslink to  $\gamma$  following reduction and exposure to conditions for ATP synthesis. Bars are labeled to indicate conditions as described for Fig. 2. Data from three separate experiments were averaged and the error bars represent standard deviations.

- Capaldi, R. A., Aggeler, R., Wilkens, S. & Gruber, G. (1996) *J. Bioenerg. Biomembr.* **28**, 397–401.
- Cross, R. L. & Duncan, T. M. (1996) *J. Bioenerg. Biomembr.* **28**, 403–408.
- Deckers-Hebestreit, G. & Altendorf, K. (1996) *Annu. Rev. Microbiol.* **50**, 791–824.
- Howitt, S. M., Rodgers, J. W., Hatch, L. P., Gibson, F. & Cox, G. B. (1996) *J. Bioenerg. Biomembr.* **28**, 415–420.
- Nakamoto, R. K. (1996) *J. Membr. Biol.* **151**, 101–111.
- Abrahams, J. P., Leslie, A. G., Lutter, R. & Walker, J. E. (1994) *Nature (London)* **370**, 621–628.
- Boyer, P. D. (1993) *Biochim. Biophys. Acta* **1140**, 215–250.
- Duncan, T. M., Bulygin, V. V., Zhou, Y., Hutcheon, M. L. & Cross, R. L. (1995) *Proc. Natl. Acad. Sci. USA* **92**, 10964–10968.
- Zhou, J.-M. & Boyer, P. D. (1993) *J. Biol. Chem.* **268**, 1531–1538.
- Weber, J., Wilke-Mounts, S., Lee, R. S.-F., Grell, E. & Senior, A. E. (1993) *J. Biol. Chem.* **268**, 20126–20133.
- Watts, S. D., Zhang, Y., Fillingame, R. H. & Capaldi, R. A. (1995) *FEBS Lett.* **368**, 235–238.
- Wilkens, S., Dunn, S. D. & Capaldi, R. A. (1994) *FEBS Lett.* **354**, 37–40.
- Lill, H., Hensel, F., Junge, W. & Engelbrecht, S. (1996) *J. Biol. Chem.* **271**, 32737–32742.
- Boyer, P. D., Cross, R. L. & Momsen, W. (1973) *Proc. Natl. Acad. Sci. USA* **70**, 2837–2839.
- Kayalar, C., Rosing, J. & Boyer, P. D. (1977) *J. Biol. Chem.* **252**, 2486–2491.
- Boyer, P. D. & Kohlbrenner, W. E. (1981) in *Energy Coupling in Photosynthesis*, eds. Selman, B. & Selman-Reiner, S. (Elsevier/North Holland, New York), pp. 231–240.
- Vik, S. B. & Antonio, B. J. (1994) *J. Biol. Chem.* **269**, 30364–30369.
- Hatch, L. P., Cox, G. B. & Howitt, S. M. (1995) *J. Biol. Chem.* **270**, 29407–29412.
- Macnab, R. M. (1996) in *Escherichia coli and Salmonella: Cellular and Molecular Biology*, ed. Neidhardt, F. C. (Am. Soc. Microbiol., Washington, DC), 2nd Ed., Vol. 1, pp. 123–145.
- Kandpal, R. P. & Boyer, P. D. (1987) *Biochim. Biophys. Acta* **890**, 97–105.
- Gogol, E. P., Johnston, E., Aggeler, R. & Capaldi, R. A. (1990) *Proc. Natl. Acad. Sci. USA* **87**, 9585–9589.
- Duncan, T. M., Zhou, Y., Bulygin, V., Hutcheon, M. L. & Cross, R. L. (1995) *Biochem. Soc. Trans.* **23**, 736–741.
- Zhou, Y., Duncan, T. M., Bulygin, V. V., Hutcheon, M. L. & Cross, R. L. (1996) *Biochim. Biophys. Acta* **1275**, 96–100.
- Sabert, D., Engelbrecht, S. & Junge, W. (1996) *Nature (London)* **381**, 623–625.
- Noji, H., Yasuda, R., Yoshida, M. & Kinosita, K., Jr. (1997) *Nature (London)* **386**, 299–302.
- Lee, R. S., Pagan, J., Wilke-Mounts, S. & Senior, A. E. (1991) *Biochemistry* **30**, 6842–6847.
- Gibson, F., Downie, J. A., Cox, G. B. & Radik, J. (1978) *J. Bacteriol.* **134**, 728–736.
- Senior, A. E., Fayle, D. R. H., Downie, J. A., Gibson, F. & Cox, G. B. (1979) *Biochem. J.* **180**, 111–118.
- Wise, J. G. (1990) *J. Biol. Chem.* **265**, 10403–10409.
- Penefsky, H. S. (1977) *J. Biol. Chem.* **252**, 2891–2899.
- Sugino, Y. & Miyoshi, Y. (1964) *J. Biol. Chem.* **239**, 2360–2364.
- Laemmli, U. K. (1970) *Nature (London)* **227**, 680–685.
- Towbin, H., Staehelin, T. & Gordon, J. (1979) *Proc. Natl. Acad. Sci. USA* **76**, 4350–4354.

34. Peterson, G. L. (1977) *Anal. Biochem.* **83**, 346–356.
35. Hermolin, J. & Fillingame, R. H. (1989) *J. Biol. Chem.* **264**, 3896–3903.
36. Nelson, N. & Taiz, L. (1989) *Trends Biochem. Sci.* **14**, 113–116.
37. Bedale, W. & Cox, M. M. (1996) *J. Biol. Chem.* **271**, 5725–5732.
38. Yu, X. & Egelman, E. H. (1997) *Nat. Struct. Biol.* **4**, 101–104.
39. Doering, C., Ermentrout, B. & Oster, G. (1995) *Biophys. J.* **69**, 2256–2267.
40. Hingorani, M. M., Washington, M. T., Moore, K. C. & Patel, S. S. (1997) *Proc. Natl. Acad. Sci. USA* **94**, 5012–5017.
41. Dombrowski, A. J., LaDine, J. R., Cross, R. L. & Platt, T. (1988) *J. Biol. Chem.* **263**, 18810–18815.
42. Story, R. M., Weber, I. T. & Steitz, T. A. (1992) *Nature (London)* **355**, 318–325.
43. Subramanya, H. S., Bird, L. E., Branningan, J. A. & Wigley, D. B. (1996) *Nature (London)* **384**, 379–383.